

# A Microfluidic Sensor Based on Meta-Surface Absorber for Rapid and Nondestructive Identification of Edible Oil Species

Jie Huang\*, Jun-Shan Li, Guo-Qing Xu, and Zhi-Hua Wei

**Abstract**—In this paper, a sensor based on a meta-surface absorber loaded with microfluidics is proposed for identification of edible oil species and provides a non-destructive, rapid, and convenient technology for the measured samples. First, a narrow-band absorber with absorption frequency of 9.887 GHz and Q value of 147, which is implemented with four W-shaped meander line resonators, is designed by Finite Element Method. Its corresponding electromagnetic resonance mechanism is explored to reveal absorption characteristics, build its corresponding equivalent circuit model, and guide the design of the palindromic microfluidic channel. The sensor shows a high sensitivity of 500 MHz/ $\epsilon'_r$ , and the corresponding sensing performance is experimentally validated by the fact that the distinguishable resonance absorption frequency shift is 461 MHz, 458 MHz, 449 MHz, 444 MHz, and 436 MHz when rapeseed oil, corn oil, peanut oil, sesame oil, and olive oil are loaded into the microfluidic channel, respectively. The identification is successfully achieved according to the resonance absorption frequency shift. Moreover, a good agreement between the simulated and measured results demonstrates that the proposed meta-surface-inspired sensor is a promising candidate to monitor and determine the quality of edible oil to some extent, and is relatively valuable to the modern agriculture and food industry.

## 1. INTRODUCTION

Edible oils are an important source of energy and essential fatty acids, have become an essential part of human daily diet, and are also widely used in food industry [1, 2]. With the improvement of quality of life, more and more attentions are paid to the quality of edible oils. In China, these edible oils, such as rapeseed oil, palm oil, peanut oil, olive oil, corn oil, account for the majority of the edible oil market. However, the price difference between them is relatively large. Due to the indistinguishable color and smell between them, adulterated and imitated edible oil frequently appear on the market for the purpose of obtaining huge profits, which will pose a serious threat to the health of consumers. Therefore, it is necessary to build a rapid and non-destructive method with the properties of micro sampling to detect these oils [2].

In most of the recent studies, different traditional technologies, such as gas chromatography method [3], evaporation and distillation [4], near infrared spectrum [5], and voltammetric electronic tongue [6], are used to detect the quality of oil. Although these technologies are very precise, they are complicated to operate and consume a large amount of sample [7]. Recently, because a substance can be characterized by its unique permittivity, a new technology, based on the dielectric characterization and perturbation theory [8], have aroused considerable enthusiasm and shows great potential in the areas of chemicals [9, 10], agriculture [11, 12], and biomedical [13–15]. As one of the typical representatives of this technology, meta-surface-inspired sensor is a potential candidate for detecting the type and quality of edible oils as it has been applied to successfully detect liquid chemicals [16–18], engine lubricant [19], transformer oil [20], edible oil [12, 21], and fuel [22]. For the detection of liquid,

---

Received 16 August 2019, Accepted 6 October 2019, Scheduled 26 October 2019

\* Corresponding author: Jie Huang (jiehuang@swu.edu.cn).

The authors are with the College of Engineering and Technology, Southwest University, Chongqing 400715, China.

conventional meta-surface sensor usually needs to be immersed in a large amount of liquid sample [23] or loaded by a capillary filled with liquid sample [24]. However, wastefulness of sample and relative low sensitivity are the main technical problems corresponding to these methods [25]. Fortunately, the emerging microfluidic technology can be used as an effective method to solve these problems. The micro-sample can be accurately placed in the strong electric field induced by a sensor by microfluidic method, which enhances the feasibility of operating with fluid medium and promotes a wider range of liquids detection [25, 26]. These features make the microfluidics a promising candidate for liquid dielectric properties analysis. Hence, as a rapid and non-destructive method, a metasurface-inspired sensor, combining meta-surface absorber owning near perfect resonance absorption characteristics and microfluidic technology, is proposed here to try to identify the type of five edible oils.

In this paper, we present a microfluidic sensor based on meta-surface absorber for rapid and non-destructive detection, which is very effective for identifying the type of edible oils. When rapeseed oil, corn oil, peanut oil, sesame oil, and olive oil are loaded into the microfluidic channel of the proposed sensor, the sensor has resonance absorption frequency shifts of 461 MHz, 458 MHz, 449 MHz, 444 MHz, and 436 MHz, respectively. These frequency shifts are relative to the resonance absorption frequency of the sensor loaded with air in the microfluidic channel. The maximum sensitivity of the sensor is  $500 \text{ MHz}/\varepsilon'_r$  ( $\varepsilon'_r$  is the real part of dielectric constant) when it is loaded by material in its sensitive areas. Finally, according to the frequency shift generated by the sensor, this sensor could successfully distinguish the species of edible oils from the experimental verification. In summary, the proposed sensor based on meta-surface absorber provides an available technological solution for the classification and detection of edible oils.

## 2. DESIGN OF SENSOR

### 2.1. Design and Analysis of Absorber

The meta-surface absorber, shown in Fig. 1(a), consists of a resonator and a metallic ground film that are divided by a dielectric substrate. The resonator is implemented by four W-shaped metallic patterns in top layer. The dielectric substrate is Rogers 5880 with complex permittivity of  $22(1 + i0.0009)$ . The pattern and film are fabricated by copper with the conductivity of  $\sigma = 5.8 \times 10^7 \text{ S/m}$ . The simulated structural parameters are presented in follows:  $P = 10.16 \text{ mm}$ ,  $L = 22.86 \text{ mm}$ ,  $W = 0.5 \text{ mm}$ ,  $s = 0.175 \text{ mm}$ ,  $g = 0.275 \text{ mm}$ ,  $L_1 = 1.9125 \text{ mm}$ ,  $L_2 = 2.1213 \text{ mm}$ ,  $L_3 = 1.45 \text{ mm}$ ,  $t = 0.035 \text{ mm}$ ,  $H = 0.4 \text{ mm}$ .

The simulation can be obtained by Finite Element Method (FEM), where a normal incident plane

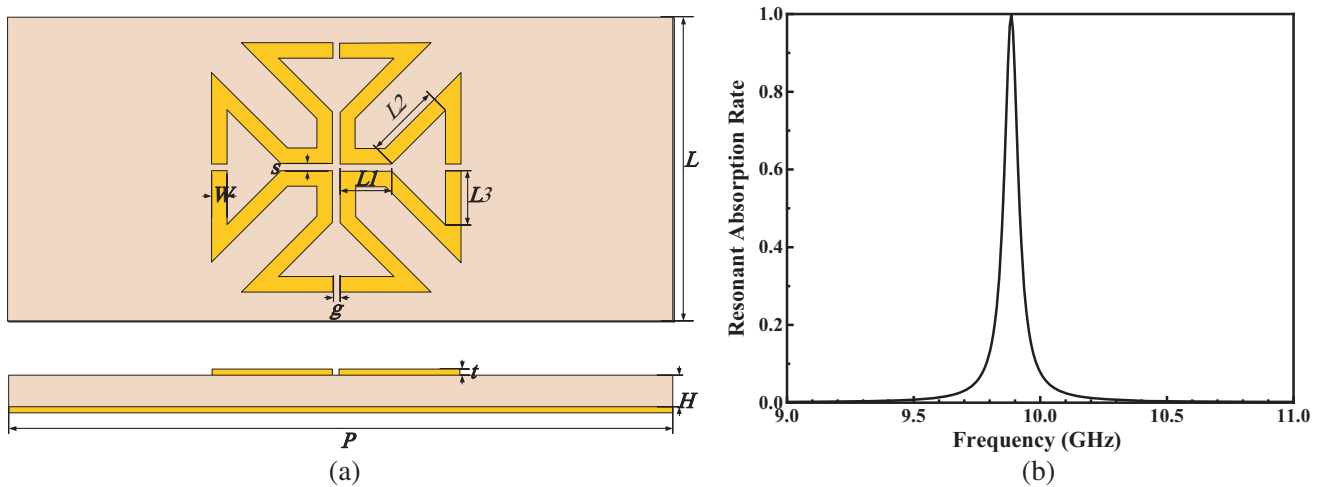


**Figure 1.** (a) The front view and lateral view of the unit cell. (b) The resonance absorption spectrum of the proposed absorber.

wave as the exciting source is utilized, and the electric field is polarized along the  $y$ -axis. The absorptivity rate can be calculated by the formula  $A(\omega) = 1 - R(\omega) - T(\omega)$ , where  $R(\omega)$  and  $T(\omega)$  are the reflection and transmission power coefficients with the expressions of  $R(\omega) = |S_{11}(\omega)|^2$  and  $T(\omega) = |S_{21}(\omega)|^2$ , respectively. The Transmission coefficient  $S_{21}(\omega)$  is approximately equal to zero because the metal thickness in the bottom layer is far thicker than its skin depth, and then the calculation express can be reduced to  $A(\omega) = 1 - R(\omega)$ . The corresponding absorption spectrum is presented in Fig. 1(b), where the absorber shows a single absorption peak at 9.887 GHz with the absorption rate over 99% and Q value of 147.

The distributions of the electric field ( $|E|$ ) of the absorber is shown in Fig. 2(a), where electric field has a high symmetry about its four symmetrical planes, and a strong electric field is generated around two vertical gaps between adjacent W-shaped resonators and on two ends of every W-shaped resonator. The power loss density distributions in the interface between the metal resonator and dielectric substrate along the vertical and horizontal plane is also shown in Fig. 2(b), where it can be found that the maximum power loss takes place in the interface and that the incident EM power is totally dissipated in the dielectric substrate. Therefore, it is suggested that the microfluidic channel loading the measured materials should be closer to the metal resonator and should be confined in the power loss region, resulting in a stronger absorption and interaction between the electrical field and material under test.

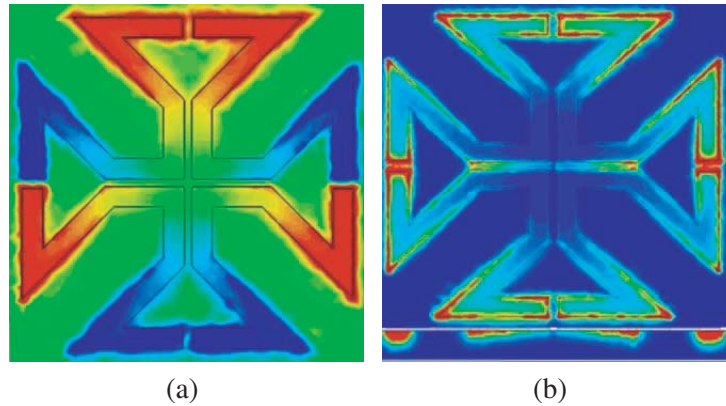


**Figure 2.** (a) Electric field distribution. (b) Energy loss distribution.

In order to explore the dependence of the resonance absorption frequency of the absorber on the permittivity of the dielectric substrate, we investigate its corresponding LC equivalent circuit model where the influence of impedance is ignored. L (inductance) is generated by the W-shaped metallic pattern, and C (capacitance) is generated by the gap between adjacent W-shaped metallic patterns, as shown in Fig. 3. The inductance and capacitance can be calculated by Eq. (1) as follows [27, 28],

$$L = \frac{\mu_0 l}{\pi} \log \left( \frac{2t}{a} \right) \quad (1a)$$

$$C = \varepsilon_0 \varepsilon_e \pi / \log \left( \frac{s}{2a} \right) \quad (1b)$$

$\mu_0$  and  $\varepsilon_0$  are the permeability and permittivity of free space;  $a$  and  $t$  represent the width and thickness of metallic patterns;  $s$  is the gap distance between adjacent metallic patterns;  $l$  is the length of metallic pattern;  $\varepsilon_e$  is the effective permittivity of dielectric substrate and can be given as:

$$\varepsilon_e = \frac{\varepsilon_r + 1}{2} + \frac{\varepsilon_r - 1}{2\sqrt{1 + 12\frac{H}{t}}}, \quad (2)$$

where  $\varepsilon_r$  and  $H$  are the relative permittivity and thickness of dielectric substrate, respectively. Finally, the parameters of lumped elements are extracted as  $L_1 = 2.2$  nH,  $L_2 = 2.2$  nH,  $C_1 = 11.93$  fF, and  $C_2 = 58.87$  fF. The validity of the model extraction method can be demonstrated by the good agreement

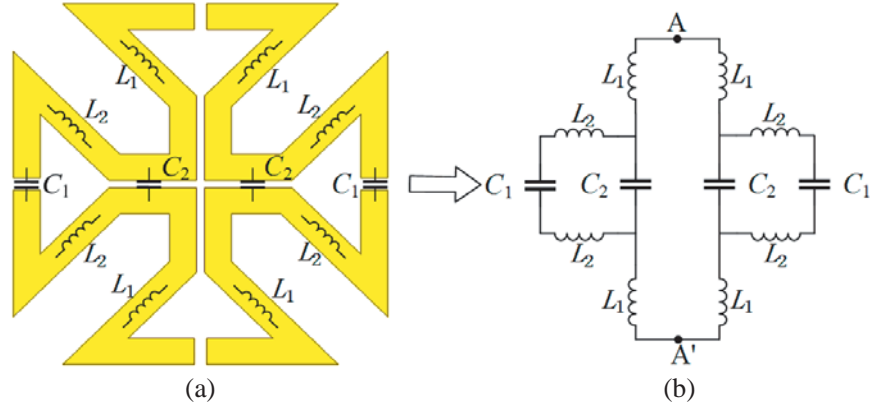


**Figure 3.** (a) Equivalent diagram of capacitance and inductance. (b) Equivalent circuit model.

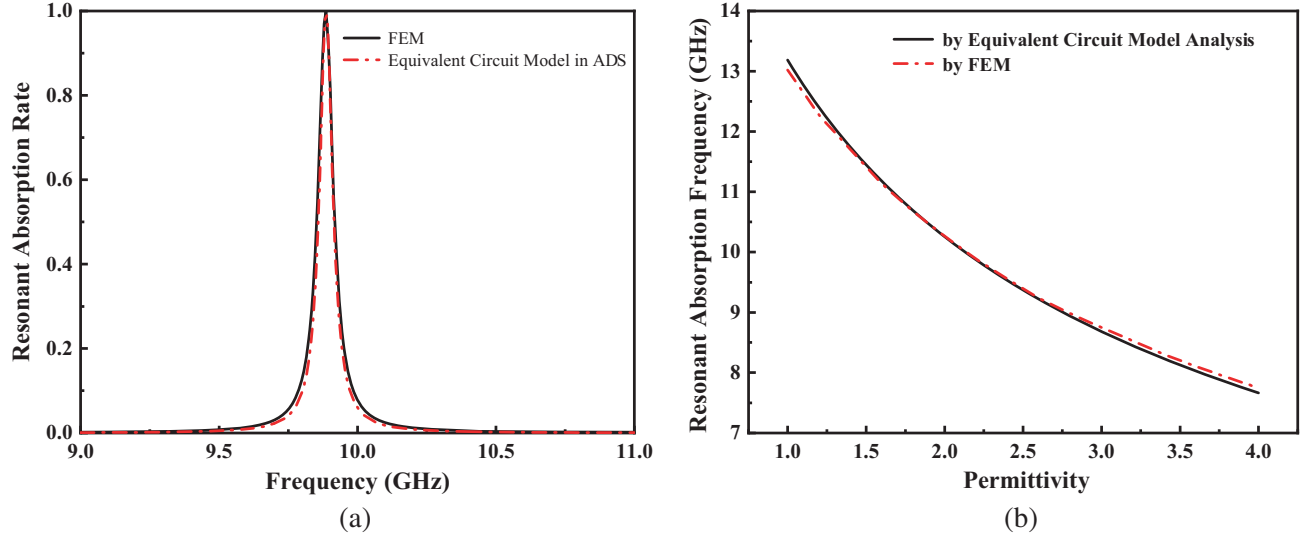


**Figure 4.** (a) Resonance absorption spectrum achieved by FEM and equivalent circuit mode in ADS. (b) The relationship between resonance absorption frequency and permittivity obtained by equivalent circuit model formula and by FEM.

between the resonance absorption rate of the absorber obtained by FEM and the one by equivalent circuit model in the soft Advanced Design System (ADS), as shown in Fig. 4(a).

The impedance expression of the absorber shown in Fig. 3(b) can be written in Eq. (3) as follows.

$$Z = j \frac{2\omega^2 L (2C_1 + C_2 - 2\omega^2 C_1 C_2 L) - 1}{\omega(C_1 + C_2 - 2\omega^2 C_1 C_2 L)} \quad (3)$$

If  $Z = 0$ , the resonance absorption frequency can be obtained in Eq. (4) as follows

$$\omega = \sqrt{\frac{2C_1 + C_2 - \sqrt{4C_1^2 + C_2^2}}{4C_1 C_2 L}} \quad (4)$$

Bring Eqs. (1)–(2) into Eq. (4), the calculated relationship between the absorption frequency and the permittivity is then available. Then, the calculated result by equivalent circuit model analysis is compared with the one by FEM, and a good agreement between them is achieved and shown in Fig. 4(b). As the permittivity of the dielectric substrate increases, the resonance absorption frequency gradually decreases. Therefore, it is suggested that the microfluidic channel can be utilized to change the permittivity of the measured material, resulting in the resonance absorption frequency shift.

### 2.2. Design of Microfluidics and Sensor

As mentioned above, sensing the resonance absorption frequency shift to edible oils can be realized by use of microfluidics technology. The absorber is divided into two parts with the same thickness of  $H_2$ , and then the microfluidics are embedded between them to implement the sensor, as shown in Fig. 5(a). According to the perturbation theory [8, 29], microfluidic channel should be placed in the strongest electric field region of the absorber, such as the interface between the metal resonator and dielectric substrate, in order to obtain better sensing performance. It is validated by the electrical field at the cross section presented in Fig. 5(b), where the microfluidics is in the strong electric field region. Limited by the process technology level, the minimum thickness  $H_2$  of 0.127 mm can be implemented. The material of microfluidics is selected as Polymethyl methacrylate (PMMA), and its relative permittivity is  $2.2(1 + i0.04)$ . The geometric parameters of microfluidics are shown as follows: microfluidic channel depth  $D = 0.35$  mm, microfluidic channel width  $U = 0.35$  mm, space between microfluidic channels  $V = 0.25$  mm, and microfluidic channel thickness  $H_1 = 0.8$  mm, number of turns  $n = 7$ .

Figure 6(a) shows the simulated spectrum of the absorption peak of the sensor varying with permittivity of material loaded in the microfluidic channel. It is clear that the resonance absorption

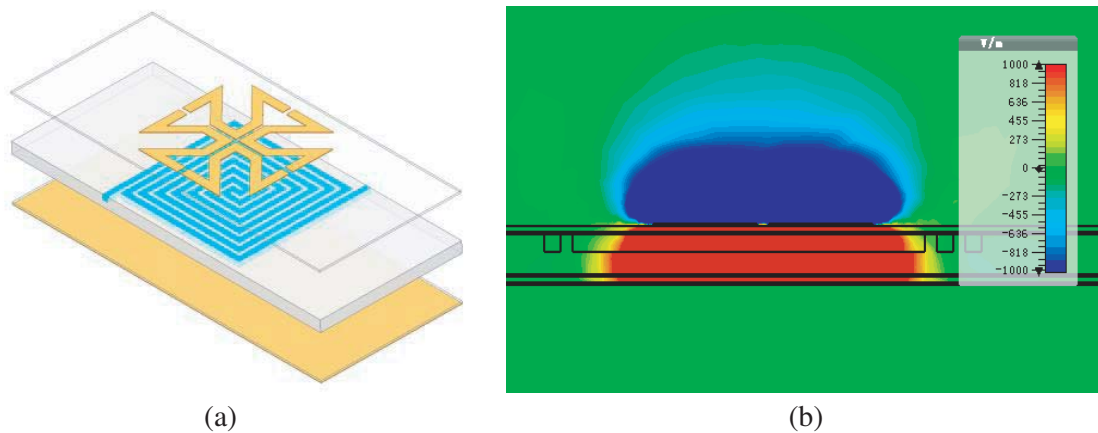


Figure 5. (a) Schematic diagram of sensor. (b) Distribution of electric field in the cross section.

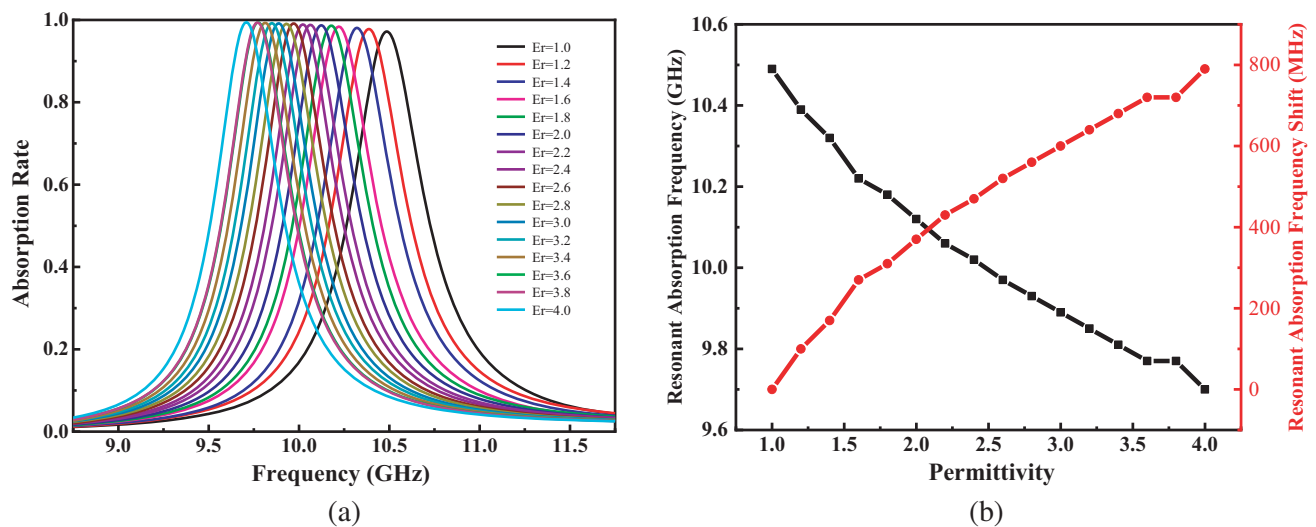


Figure 6. (a) Spectrum of the absorption peak of the sensor varying with permittivity. (b) Resonance absorption frequency of the designed sensor as a function of permittivity.

frequency has a redshift with the increase of permittivity. This phenomenon is consistent with the sensing mechanism analyzed above. Namely, the increase of permittivity results in a stronger perturbation to the induced electric field of the sensor and finally generates a larger frequency shift. Fig. 6(b) shows the simulated quantitative relationship between them. When permittivity increases from 1 to 4, the resonance absorption frequency is monotonically reduced from 10.49 GHz to 9.70 GHz, reaching the frequency shift of 0.79 GHz. Relative to the resonance absorption frequency of the sensor loaded by air in the microfluidic channel, the relative frequency shift performance is also shown in Fig. 6(b) in red. These results demonstrate that the sensor proposed here can effectively detect the liquid whose permittivity is in the range from 1 to 4.

### 3. FABRICATION, MEASUREMENT AND DISCUSSION

#### 3.1. Sensor Fabrication and Measurement Setup

To experimentally verify its sensing performances of the sensor proposed here, the proposed meta-surface absorber and microfluidics are fabricated by standard print circuit board (PCB) technology and micromachining processes, respectively. The absorber is manufactured separately by the upper and lower parts, and then is integrated with the microfluidics to form the sensor, as illustrated in Fig. 7(a). In order to avoid the leakage of edible oil, the microfluidics is embedded between them and is bonded to the upper and lower parts of the absorber by use of an insulated bonding film. Two via holes are dug on the surface of the upper part to connect the microfluidic channel. In addition, two PEEK interface bases with injection catheters are fixed on the via-holes by use of AB glue in order to inject edible oil into the microfluidic channel. Finally, a photograph of the assembled sensor prototype is show in Fig. 7(b).

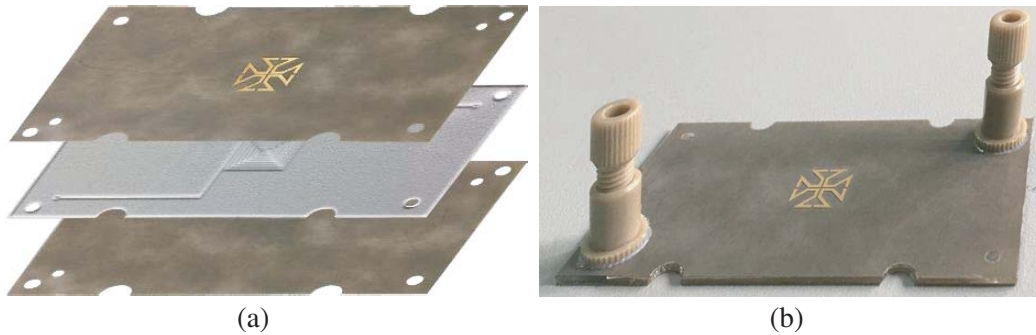


**Figure 7.** Photographs of the designed sensor. (a) Assembly process. (b) Physical structure.

In order to measure the absorptivity of the proposed sensor, the measurement setup by use of waveguide is built, as shown in Fig. 8. Two WR-90 waveguide adapters are connected to a vector network analyzer (Agilent E5071C), and the sensor prototype is embedded between the two waveguide adapters. Then, edible oils are injected into microfluidic channel using a syringe, and the reflection coefficients  $S_{11}$  is measured to calculate the absorptivity spectrum by an expression previously defined of  $A(w) = 1 - |S_{11}(w)|^2$ . Note that the inject rate should be relatively slow and keep constant; otherwise, it may cause problems, such as air bubbles or uneven filling. Additionally, to eliminate the effect of the previous residue on the current result, deionized water should be injected into the microfluidic channel by a syringe to clean the residues several times. Then it is immediately followed that dry air is injected to remove residual water droplets in the microfluidic channel until the resonance absorption frequency returns to the one in empty state. All the measurements are performed at room temperature.

#### 3.2. Results and Discussions

Figure 9 shows the measured reflection coefficients  $S_{11}$  of the designed sensor loaded by air and five types of edible oils. The resonance peak is at 10.481 GHz when the microfluidic channel is



Figure 8. Photograph of the experimental setup.

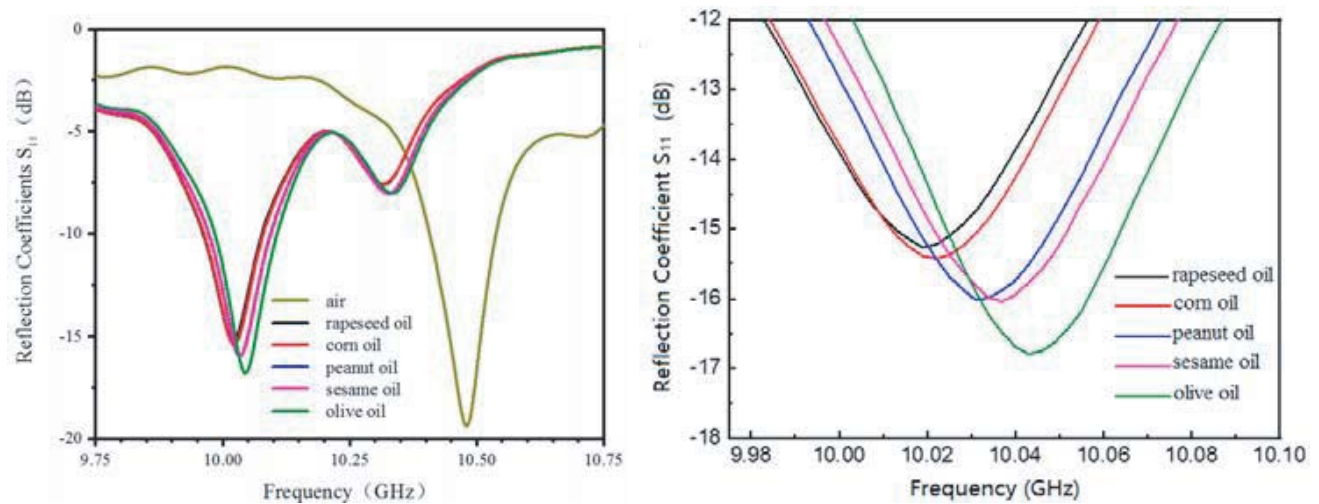


Figure 9. Measured reflection coefficient  $S_{11}$  of the sensor loaded by air and five edible oils.

filled with air. When rapeseed oil, corn oil, peanut oil, sesame oil, and olive oil are injected into the microfluidic channel, the corresponding resonance peak frequencies are 10.02 GHz, 10.023 GHz, 10.032 GHz, 10.037 GHz, and 10.045 GHz, respectively. Relative to the resonance peak of the sensor in the empty state, the corresponding relative resonance frequency shifts are 461 MHz, 458 MHz, 449 MHz, 444 MHz, and 436 MHz, respectively. Moreover, the maximum relative resonance frequency difference between these edible oils is up to 25 MHz, and the minimum one is up to 3 MHz, which is much larger than the frequency resolution of the vector network analyzer E5071C. And the corresponding maximum sensitivity is competitively up to  $500 \text{ MHz}/\epsilon'_r$ . A comparison of sensing performances is made between other recently reported sensors and the sensor proposed here, and is listed in Table 1, where it is observed that the proposed sensor shows higher sensitivity. As shown in Fig. 6(b), it can be concluded that the bigger the permittivity is, the larger the resonance frequency shift is, and vice versa. Therefore, we can judge from the measured results that the dielectric constant relationship among five types of edible oils is as follows:  $\epsilon_{\text{rapeseed oil}} > \epsilon_{\text{corn oil}} > \epsilon_{\text{peanut oil}} > \epsilon_{\text{sesame oil}} > \epsilon_{\text{olive oil}}$ . Moreover, this dielectric constant relationship has also been further verified by the measured dielectric dispersion spectrum of these edible oils using coaxial probe kit (N1500A, Keysight, Chengdu, China) in the frequency range from 8 GHz to 11 GHz, as shown in Fig. 10. Thus, it can be confirmed that the designed meta-surface absorber sensor can be used to identify the type of edible oils according to the resonance frequency shift.

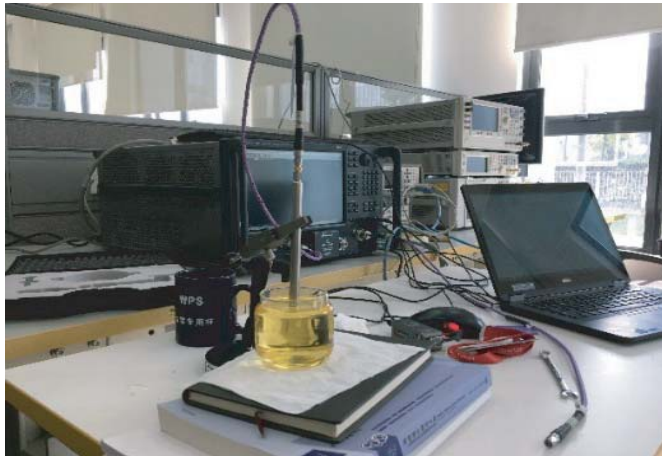
In order to verify the reliability of the sensor design, these measured dielectric dispersion

characteristics of these five types of edible oils are embedded into the FEM electromagnetic simulator to obtain the simulated reflection coefficients  $S_{11}$ . Fig. 11 shows the simulated and measured results when the microfluidic channel is loaded by air and sesame oil. It can be seen that the measured result is in good agreement with the simulated ones except a tiny frequency deviation and a minor decrease in return loss. The frequency deviation could be mainly attributed to the imprecise dielectric constant of actual substrate and microfluidic material, and partly to the fabrication tolerance of PCB and micromachining processes. The amplitude decrease may be caused by the losses incurred from the substrate or the insulated bonding film sandwiched by dielectric substrates and the microfluidics.

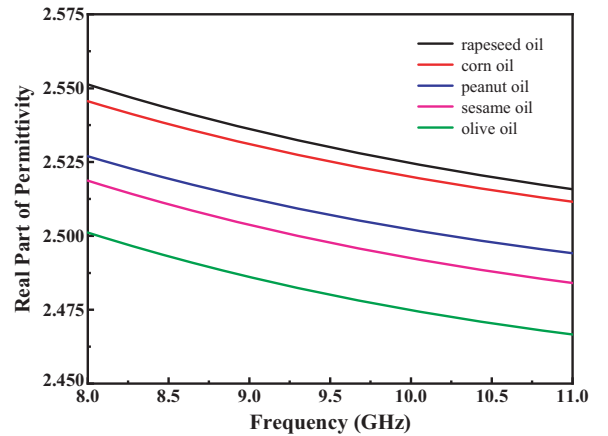
**Table 1.** Comparison of other recently published works and this work.

Ref.	Sensor Structure	Sensing Material	Operating Frequency in the empty state (GHz)	$\epsilon_r$	Frequency Shift ( $f$ ) [MHz]	Sensitivity ( $f/\epsilon_r$ ) <sup>†</sup>
[30]	CSRR-based resonator	Ethanol liquid	4.16	1–5.5	270	49.1 MHz/ $\epsilon_r'$
[31]	EBG-inspired Patch resonator	Mixture of Fish oil and Olive oil	2.592	2.6–2.834	48	205.1 MHz/ $\epsilon_r'$
[32]	Metamaterial absorber	Ethanol liquid	12.12	(1–6.5) $\S$	660	120 MHz/ $\epsilon_r'$
[33]	Circular SIW resonator	Ethanol purity	5.35	1–6.5	380	69.07 MHz/ $\epsilon_r'$
This work	Meta-surface absorber	Edible oils	10.49	2.5–2.55	25	500 MHz/ $\epsilon_r'$

<sup>†</sup>  $\epsilon_r'$  represents unit dielectric constant,  $\S$   $\epsilon_r$  of ethanol is assumed to be 6.5



(a)



(b)

**Figure 10.** (a) Measurement setup, (b) the measured dielectric dispersion spectrum of five types of edible oils.

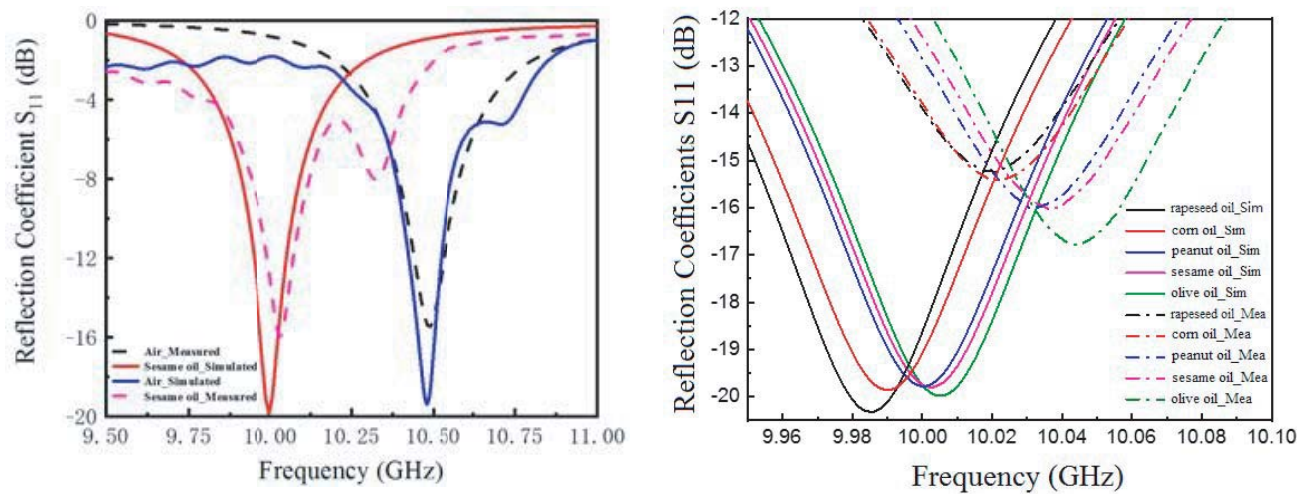


**Figure 11.** Contrast chart of simulated and measured results of the sensor load by air and five edible oils.

However, the consistent trends in both simulated and measured reflection spectrums that the resonance frequency has red shifts with the increase of permittivity further demonstrate the validity in the process of design.

#### 4. CONCLUSION

In this paper, a microfluidic sensor, based on a meta-surface absorber for identifying of edible oil species, is demonstrated both numerically and experimentally. The absorber, implemented by four W-shaped meander line resonators, has a resonance absorption frequency of 9.887 GHz and Q value of 147. The electric field distribution, equivalent circuit model, and mathematical mode quantitatively relating the resonance absorption frequency of the sensor and the permittivity of dielectric substrate are theoretically established to reveal the sensing mechanism and guide the design of microfluidic channel. The resonant frequency shift reaches 0.79 GHz when the permittivity of liquid loaded in the microfluidic channel is in the range from 1 to 4. Then the absorber is manufactured separately by the upper and lower parts, and they are integrated with the microfluidics to form the sensor proposed here. Finally, the sensor shows a relatively high sensitivity of  $500 \text{ MHz}/\epsilon'_r$ , and the corresponding sensing performance is experimentally verified by using waveguide test method. When rapeseed oil, corn oil, peanut oil, sesame oil, and olive oil are loaded into the microfluidic channel of the proposed sensor, the relative resonance frequency shift is used as the signature of the sensor for identification of edible oil species, characterized by their unique dielectric dispersion spectrums. The microfluidics-based sensing concept also makes the proposed sensor non-invasive, contactless, and reusable, and may have potential applications in many areas such as biological, food, and pharmaceutical industry.

#### ACKNOWLEDGMENT

This work was supported in part by the National Natural Science Foundation of China (Grant No. 61401373 and No. 61971358), in part by the Fundamental Research Funds for the Central Universities (Grant No. XDJK2018B017 Grant No. XDJK2019D016), and in part by the Research Fund for the Doctoral Program of Southwest University (Grant No. SWU111030).

## REFERENCES

1. Jakoby, B., G. Art, and J. Bastemeijer, "Novel analog readout electronics for microacoustic thickness shear-mode sensors," *IEEE Sensor Journal*, Vol. 5, No. 5, 1106–1111, 2005.
2. Hou, X. W., G. L. Wang, G. Q. Su, X. Wang, and S. D. Nie, "Rapid identification of edible oil species using supervised support vector machine based on low-field nuclear magnetic resonance relaxation features," *Food Chemistry*, Vol. 280, 139–145, 2019.
3. Alberdi-Cedeno, J., M. L. Ibargoitia, and M. D. Guillen, "Monitoring of minor compounds in corn oil oxidation by direct immersion-solid phase microextraction-gas chromatography/mass spectrometry. New oil oxidation markers," *Food Chemistry*, Vol. 290, 286–294, 2019.
4. Larsson, W., J. Jalbert, R. Gilbert, and A. Cedergren, "Efficiency of methods for Karl Fischer determination of water in oils based on oven evaporation and azeotropic distillation," *Analytical Chemistry*, Vol. 75, No. 6, 1227–1232, 2003.
5. Holland, T., A. M. Abdul-Munaim, D. G. Watson, and P. Sivakumar, "IP. Simportance of emulsification in calibrating infrared spectrosopes for analyzing water contamination in used or in-service engine oil," *Lubricants*, Vol. 6, No. 2, 35, 2018.
6. Niu, Q., S. S. Chen, L. Wang, Y. B. Hui, and Q. Wang, "Research of edible oil detection and variety distinguish based on voltammetric electronic tongue," *IEEE International Conference on Information and Automation*, Lijiang, China, August 2015.
7. Larsson, W., J. Jalbert, R. Gilbert, and A. Cedergren, "Efficiency of methods for Karl Fischer determination of water in oils based on oven evaporation and azeotropic distillation," *Analytical Chemistry*, Vol. 75, No. 6, 1227–1232, 2003.
8. Pozar, D. M., *Microwave Engineering*, 3rd Edition, John Wiley & Sons, 2005.
9. Joshi, K. K. and R. D. Pollard, "Sensitivity analysis and experimental investigation of microstrip resonator technique for the in-process moisture/permittivity measurement of petrochemicals and emulsions of crude oil and water," *Proceedings of the 2006 IEEE MTT-S International Microwave Symposium Digest*, San Francisco, CA, USA, June 2006.
10. Agarwal, S. and Y. K. Prajapati, "Multifunctional metamaterial surface for absorbing and sensing applications," *Optics Communications*, Vol. 439, 304–307, 2019.
11. Nigmatullin, R. R., A. A. Arbuzov, S. O. Nelson, and S. Trabelsi, "Dielectric relaxation in complex systems: Quality sensing and dielectric properties of honeydew melons from 10 MHz to 1.8 GHz," *Journal of Instrumentation*, Vol. 1, P10002, 2006.
12. Tiwari, N. K., S. P. Singh, and M. J. Akhtar, "Novel improved sensitivity planar microwave probe for adulteration detection in edible oils," *IEEE Microwave and Wireless Components Letters*, Vol. 29, No. 2, 164–166, 2019.
13. Gregory, A. P. and R. N. Clarke, "A review of RF and microwave techniques for dielectric measurements on polar liquids," *IEEE Transactions on Dielectrics and Electrical Insulation*, Vol. 13, No. 4, 727–743, 2006.
14. Jamal, F. I., S. Guha, H. M. Eissa, S. Vehring, D. Kissinger, and C. Meliani, "K-band BiCMOS based near-field biomedical dielectric sensor for Detection of fat and calcium in blood," *2015 European Microwave Conference (EuMC)*, Paris, France, September 2015.
15. Di Meo, S., et al., "Correlation between dielectric properties and women age for breast cancer detection at 30 GHz," *2018 IEEE International Microwave Biomedical Conference (IMBioC)*, 190–192, Philadelphia, PA, USA, June 14–15, 2018.
16. Abdulkarim, Y. I., L. W. Deng, O. Altıntaş, E. Unal, and M. Karaaslan, "Metamaterial absorber sensor design by incorporating swastika shaped resonator to determination of the liquid chemicals depending on electrical characteristics," *Physica E: Low-dimensional Systems and Nanostructures*, Vol. 114, 113593, 2019.
17. Liu, C. J. and Y. Pu, "A microstrip resonator with slotted ground plane for complex permittivity measurements of liquid," *IEEE Microwave Wireless Components Letters*, Vol. 18, No. 4, 257–259, 2008.
18. Tiwari, N. K., S. Tiwari, and M. J. Akhtar, "Design of CSRR-based electronically tunable compact

- RF sensor for material testing,” *IEEE Sensors Journal*, Vol. 18, No. 18, 7450–7457, 2018.
19. Altintas, O., M. Aksoy, E. Unal, O. Akgol, and M. Karaaslan, “Artificial neural network approach for locomotive maintenance by monitoring dielectric properties of engine lubricant,” *Measurement*, Vol. 145, 678–686, 2019.
  20. Altintas, O., M. Aksoy, E. Unal, and M. Karaaslan, “Chemical liquid and transformer oil condition sensor based on metamaterial-inspired labyrinth resonator,” *Journal of The Electrochemical Society*, Vol. 166, No. 6, B482–B488, 2019.
  21. Kumar, A. V. P., et al., “Dielectric characterization of common edible oils in the higher microwave frequencies using cavity perturbation,” *Journal of Microwave Power and Electromagnetic Energy*, Vol. 53, No. 1, 48–56, 2019.
  22. Tumkaya, M. A., F. Dincer, M. Karaaslan, and C. Sabah, “Sensitive metamaterial sensor for distinction of authentic and inauthentic fuel samples,” *Journal of Electronic Materials*, Vol. 46, No. 8, 4955–4962, 2017.
  23. Liu, C. J. and Y. Pu, “A microstrip resonator with slotted ground plane for complex permittivity measurements of liquid,” *IEEE Microwave Wireless Components Letters*, Vol. 18, No. 4, 257–259, 2008.
  24. Abduljabar, A. A., D. J. Rowe, A. Porch, and D. A. Barrow, “Novel microwave microfluidic sensor using a microstrip split-ring resonator,” *IEEE Transactions on Microwave Theory and Techniques*, Vol. 62, No. 3, 679–688, 2014.
  25. Wei, Z. H., et al., “A high-sensitivity microfluidic sensor based on square SIW re-entrant cavity for complex permittivity measurement of Liquids,” *Sensors*, Vol. 18, No. 11, 4005, 2018.
  26. Ling, K., et al., “Microfluidic tunable inkjet-printed metamaterial absorber on paper,” *Optics Express*, Vol. 23, No. 1, 110–120, 2015.
  27. Pang, Y. Q., H. F. Cheng, Y. J. Zhou, and J. Wang, “Analysis and design of wire-based metamaterial absorbers using equivalent circuit approach,” *Journal of Applied Physics*, Vol. 113, No. 11, 114902, 2013.
  28. Zhou, J. F., E. N. Economou, T. Koschny, and C. M. Soukoulis, “Unifying approach to left-handed material design,” *Optics Letters*, Vol. 31, No. 24, 3620–3622, 2006.
  29. Gao, C., T. Wei, F. Duewer, Y. L. Lu, and X. D. Xiang, “High spatial resolution quantitative microwave impedance microscopy by a scanning tip microwave near-field microscope,” *Applied Physics Letters*, Vol. 71, No. 13, 1872–1874, 1997.
  30. Salim, A. and S. J. Lim, “Complementary split-ring resonator-loaded microfluidic ethanol chemical sensor,” *Sensors*, Vol. 16, 1802, 2016.
  31. Yadav, R. and P. N. Patel, “Experimental study of adulteration detection in fish oil using novel PDMS cavity bonded EBG inspired patch sensor,” *IEEE Sensors Journal*, Vol. 16, No. 11, 4354–4361, 2016.
  32. Yoo, M. Y., H. K. Kim, and S. J. Lim, “Electromagnetic-based ethanol chemical sensor using metamaterial absorber,” *Sensors and Actuators B: Chemical*, Vol. B222, 173–180, 2016.
  33. Memon, M. U. and S. J. Lim, “Microfluidic high-Q circular Substrate-Integrated Waveguide (SIW) cavity for Radio Frequency (RF) chemical liquid sensing,” *Sensors*, Vol. 18, 143, 2018.